A Secreted WNT-Ligand Binding Domain of FZD5 Generated by a Frameshift Mutation Causes Autosomal Dominant Coloboma

HMG Advance Access published January 24, 2016

A Secreted WNT-Ligand Binding Domain of FZD5 Generated by a Frameshift Mutation Causes Autosomal Dominant Coloboma

Chunqiao Liu[1,2,#], Sonya A. Widen[3,#], Kathleen A. Williamson[4,#], Rinki Ratnapriya[1], Christina Gerth-Kahlert[5], Joe Rainger[4], Ramakrishna P. Alur[6], Erin Strachan[7], Souparnika H. Manjunath[1], Archana Balakrishnan[1], James A. Floyd[8], UK10K Consortium[8], Tiansen Li[1], Andrew Waskiewicz[3,*], Brian Brooks[6], Ordan J. Lehmann[7,9,*], David R. FitzPatrick[4,*], and Anand Swaroop[1,*]

[1]Neurobiology-Neurodegeneration & Repair Laboratory, National Eye Institute, National Institutes of Health, 6 Center Drive, Bethesda, MD 20892, USA

[2]State Key Laboratory of Ophthalmology, Zhongshan Ophthalmic Center, Sun Yat-sen University, Guangzhou 510060, China

[3]Department of Biological Sciences, University of Alberta, Edmonton, AB T6G 2E9, Canada

[4]MRC Human Genetics Unit, Institute of Genetic and Molecular Medicine, University of Edinburgh, Edinburgh EH4 2XU, UK

[5]Dept. of Ophthalmology, University Hospital Zurich, Frauenklinikstrasse 24, 8091 Zurich, Switzerland

[6]Unit on Pediatric, Developmental, and Genetic Eye Disease, National Eye Institute, 10 Center Drive, Bethesda, MD 20892, USA

[7]Department of Ophthalmology and Visual Sciences, University of Alberta, Edmonton, AB T6G 2H7, Canada

[8]Welcome Trust Sanger Institute, Hinxton, Cambridge, CB10 1HH, UK

[9]Dept. of Medical Genetics, University of Alberta, Edmonton, AB T6G 2H7

*Correspondence may be addressed to: Prof. Anand Swaroop, Neurobiology-Neurodegeneration & Repair Laboratory, National Eye Institute, 6 Center Drive, Bethesda, MD 20892, USA. swaroopa@nei.nih.gov, Prof. David R. FitzPatrick, MRC Human Genetics Unit, University of Edinburgh, Western General Hospital, Edinburgh EH4 2XU, UK. david.fitzpatrick@ed.ac.uk, Prof. Ordan J. Lehmann, Department of Ophthalmology and Visual Sciences, University of Alberta, Edmonton, AB T6G 2H7, Canada. olehmann@ualberta.ca, Prof. Andrew Waskiewicz, Department of Biological Sciences, University of Alberta, Edmonton, AB T6G 2E9 Canada. aw@ualberta.ca

[#]These authors should be considered as joint first authors.

ABSTRACT

Ocular coloboma is a common eye malformation resulting from incomplete fusion of the optic fissure during development. Coloboma is often associated with microphthalmia and/or contralateral anophthalmia. Coloboma shows extensive locus heterogeneity associated with causative mutations identified in genes encoding developmental transcription factors or components of signaling pathways. We report an ultra-rare, heterozygous frameshift mutation in *FZD5* (p.Ala219Glufs*49) that was identified independently in two branches of a large family with autosomal dominant non-syndromic coloboma. *FZD5* has a single coding exon and consequently a transcript with this frameshift variant is not a canonical substrate for nonsense-mediated decay. *FZD5* encodes a transmembrane receptor with a conserved extracellular cysteine rich domain (CRD) for ligand binding. The frameshift mutation results in the production of a truncated protein, which retains the WNT-ligand binding domain but lacks the transmembrane domain. The truncated protein was secreted from cells, and behaved as a dominant-negative FZD5 receptor, antagonizing both canonical and non-canonical WNT signaling. Expression of the resultant mutant protein caused coloboma and microphthalmia in zebrafish, and disruption of the apical junction of the retinal neural epithelium in mouse, mimicking that of *Fz5/Fz8* compound conditional knockout mutants.

Our studies have revealed a conserved role of Wnt-Frizzled signaling in ocular development and directly implicate WNT-FZD signaling both in normal closure of the human optic fissure and pathogenesis of coloboma.

INTRODUCTION

Ocular coloboma (OC) is a developmental structural defect caused by the abnormal persistence of the optic fissure in post-embryonic life. In combination with microphthalmia (small eyes) and anophthalmia (absent eyes), OC represents a spectrum of malformations that account for an estimated 10% to 15% of pediatric blindness (1). Transcription factors and signaling pathways play crucial roles in optic cup morphogenesis and fissure closure (2, 3). Accordingly, human genetic studies together with vertebrate models have implicated Bone Morphogenetic Protein (BMP) (4-7), Hedgehog (Hh) (8), Retinoic Acid (RA) (9-11) and Hippo (12) pathways in the pathogenesis of these ocular malformations (8, 13-15). Defects in components of Wnt signaling have been attributed to syndromic and non-syndromic ocular diseases, including Norrie disease (16, 17), osteoporosis-pseudoglioma syndrome (18) and familial exudative vitreoretinopathy (16, 17, 19-21), but not with abnormalities associated with ocular morphogenesis.

A growing body of evidence from several vertebrate models indicates that Wnt signaling is indispensable in optic field development and ocular morphogenesis. In the Wnt pathway, non-canonical (β-catenin-independent) signaling interacts with canonical (β-catenin-dependent) signaling to control presumptive retinal versus forebrain fates (22). Loss of non-canonical ligands, Wnt5 and Wnt11, causes failure of eye field segregation (22), whereas inactivation of β-catenin prior to optic vesicle differentiation causes anophthalmia (23). At later stages of development, the canonical pathway also contributes to optic cup morphogenesis, with overexpression of the Wnt inhibitor Dkk1 leading to abnormal lens formation and coloboma (24, 25). Furthermore, loss of the Secreted Frizzled Related

Proteins (sFRPs; known modulators of Wnt signaling) causes defects in optic cup patterning (26).

The Wnt receptor Frizzled-5 (Fzd5) mediates both canonical and non-canonical signaling (22, 27). During eye field specification, Fzd5 is specifically expressed in evaginating eye precursors (28, 29). In zebrafish, Wnt11-Fzd5 signaling promotes eye field specification using the non-canonical pathway (22). In Xenopus, Fzd5 acting via the canonical pathway controls the neural potential of retinal progenitors through regulation of Sox2 (30). Mouse *Fzd5*$^{-/-}$ mutants display extreme optic cup invagination defects with failure to induce lens formation (31), whereas conditional *Fzd5* mutants (Supplementary Fig.1) exhibit both microphthalmia and coloboma with disrupted retinal epithelial apical junctions (27, 32) implicating Fzd5 in mammalian ocular morphogenesis and early neurogenesis. Additionally, mouse knockout mutants of *Lrp6*, encoding Fzd co-receptor presumed to be in the canonical Wnt signaling pathway (33), demonstrate ocular phenotypes similar to those observed in the conditional *Fzd5* mutants. We therefore hypothesized that mutations in *FZD5* may be involved in the development of human congenital ocular malformations. In this study, we tested this hypothesis using two independent methods: an unbiased genetic screen, and a candidate gene approach. Both of these identified the same single novel frameshift mutation in *FZD5* in a large, extended family in which non-syndromic OC segregated as an autosomal dominant disorder. Functional analysis of the mutant protein, using zebrafish and mouse retinal explants, strongly suggests a dominant negative effect on WNT signaling which is likely responsible for optic fissure closure defects. The present study therefore directly implicates WNT-FZD signaling in the pathogenesis of human coloboma.

RESULTS

A frameshift mutation in *FZD5* causes automomal dominant coloboma

Whole exome sequencing (WES) was performed as part of the Rare Disease component of UK10K (www.uk10k.org) in five members of a large family with autosomal dominant OC (Family 3483; Fig. 1A-C). The affected individuals IV:6, V:1, VI:2 and VI:5 shared only one

ultra-rare variant (not present in ExAC, EVS, 1000G, UK10K internal databases); a frameshift mutation in *FZD5* (c.656delCinsAG; p.Ala219Glufs*49, hereafter referred A219Xfs*49). This variant was then shown to co-segregate with the disease in all affected individuals available for testing with one exception, IV:7 (Fig. 1A). IV:7 has bilateral coloboma but is “married-in” to the family being unrelated to the affected individuals VI:2, V:1, IV:1, IV:4 and IV:6 (his wife). He has no prior family history of eye malformations and no other plausible causative variants could be identified in his exome sequence data. Two unaffected individuals (III:2 & V:8) also carried the mutation and were considered as non-penetrant. Targeted re-sequencing of *FZD5* in an additional 380 unrelated coloboma patients from the MRC Human Genetics Unit Cohort as part of UK10K revealed no other potentially pathogenic variants.

Concurrently, *FZD5* was screened as a candidate gene, based on mouse studies (27, 32), in 172 unrelated individuals with coloboma from cohorts at National Eye Institute (NEI), USA and University of Alberta (U of A), Canada. These studies revealed the identical A219Xfs*49 mutation in all four affected individuals from family 111, where each exhibited bilateral coloboma and related phenotypes [e.g., microphthalmia, and cataract] (Fig. 1A, B).

Haplotype analysis using five microsatellite markers flanking the *FZD5* gene suggested a recent common ancestry between Family 3483 and Family 111 (Supplementary Fig. 2). Based on the information provided by family 3483 that individual II:4 had emigrated to North America, this female represented a plausible genetic link with Family 111. In addition, both families are of Mennonite ancestry and originated from the same region in Europe. For the purpose of calculating the two-point LOD score, we designated II:4 in Family 3483 as the maternal great-grandmother of individual I:2 in Family 111, which is the closest possible link based on information from Family 111. This was a conservative approach, as it would generate a minimum possible LOD score associated with co-segregation of the disease and the mutation in the combined family. The linkage analysis was performed using the R package paramlink. Co-segregation of the *FZD5* mutation with coloboma in the extended pedigree gave a two-point LOD score (θ=0) ranging from 3.9-4.2 using penetrance

values between 0.1-1. It was not possible to obtain an accurate estimate of the penetrance for this mutation as we were not able to examine or genotype all apparently unaffected individuals in both branches of the family. However, on the basis of the genotypes we can safely conclude a relatively high but incomplete penetrance of the disease mutation.

FZD5 has a single coding exon with a 5' non-coding exon. As such the A219Xfs*49 mutant transcript is not predicted to be a substrate for nonsense-mediated decay. The A219Xfs*49 mutation is thus likely to result in production of a truncated FZD5 protein with an intact highly conserved ligand-binding domain (extracellular cysteine rich domain, CRD) but lacking the seven transmembrane domains (Fig. 1D) (Supplementary Fig. 3).

Within the NEI and U of A cohorts, one additional rare missense variant was identified (c. 290A>T; p.Asp97Val (D97V); Supplementary table 1, Supplementary Fig. 4A, B). This variant is of uncertain significance as this variant was not present in the unaffected mother or brother and the father was deceased (Supplementary Fig. 4A). This mutation did not significantly change FZD5 protein level or its membrane localization by in vitro transfection assay (Supplementary Fig. 4C). Atomic non-local environment assessment (ANOLEA) predicted that the D97V variant would perturb local interactions (Supplementary Fig. 4D). Super Topflash (STF) reporter assays indicated a slight but consistent increase of Wnt9b-stimulated canonical Wnt activity by D97V mutation (Supplementary Fig. 4E) suggesting a gain-of-function.

Altered expression of FZD5 A219Xfs*49 in zebrafish results in microphthalmia and coloboma

To elucidate the functional relevance of the human FZD5 A219Xfs*49 mutation, zebrafish were used as a model system. Concordant with observations in mouse *Fzd5* mutants (27, 32), zebrafish *fzd5* morphants exhibited coloboma and microphthalmia phenotypes (Fig. 2A-D). In addition, over-expression of the FZD5-A219Xfs*49 mutant in zebrafish embryos also resulted in coloboma and microphthalmia (Fig. 2E-J). Surprisingly, these phenotypes were

more prevalent when the wild type FZD5 protein was over-expressed (Fig. 2K-L). We noted that the eye size was similar when either WT or FZD5-A219Xfs*49 mutant was over-expressed (Supplementary Fig. 5). These observations suggest that precise FZD5 and/or Wnt signaling dosage is critical for ocular development.

FZD5 A219Xfs*49 is a secreted protein that binds to Wnt but is incapable of mediating Wnt signaling

To further understand the functional consequences of the human FZD5 A219Xfs*49 mutation, we examined mutant protein expression and localization *in vitro*. Transfection of A219Xfs*49 cDNA construct into HEK293 cells produced a truncated FZD5 protein as predicted, containing the entire ligand-binding domain but not the transmembrane domains. Under non-reducing conditions, the mutant FZD5 A219Xfs*49 protein shows multiple bands in the cell extracts, including one of ~50 KD and several ~21 KD (Fig. 3A). With the addition of β–mercaptoethanol, the truncated FZD5 protein primarily migrated at a lower molecular weight in the ECM fraction (Fig. 3A). Live cell surface immunofluorescence analysis confirmed that truncated FZD5 did not localize to the outer cell membrane (in contrast to the full length FZD5) and instead displayed punctate and/or irregular extracellular staining (Fig. 3B, Supplementary Fig. 6). As predicted, the A219Xfs*49 truncated FZD5 protein abrogated the ability to mediate both canonical (Fig. 3C, integrated TCF-dependent reporter) and non-canonical WNT signaling activities (Fig. 3D, pulldown assay of Wnt5a stimulated GTP-RhoA). An engineered secreted FZD5-CRD protein (sCRD, fused with human Ig-Fc fragment) had an effect similar to the A219Xfs*49 FZD5 mutant (Fig. 3C, D), suggesting that the secretion of the latter is critical for its abnormal function. To examine whether A219Xfs*49 FZD5 binds to Wnt, co-IP experiments were conducted using cell extracts transfected with *Wnt3a-myc, WNT7A-HA, FZD5* and *FZD5 A219Xfs*49* constructs in different combinations (34, 35). We detected binding of FZD5 A219Xfs*49 to WNT7A as well as FZD5 (Supplementary Fig. 7), suggesting that a competition may exist between A219Xfs*49 FZD5 mutant and wild type for WNT utilization.

FZD5 A219Xfs*49 antagonizes both canonical and non-canonical Wnt signaling

Given the abnormal function of truncated *FZD5 A219Xfs*49*, as indicated by its aberrant localization at the plasma membrane, and that A219Xfs*49 was associated with a dominant mode of inheritance in Family 3483 and Family 111, we reasoned that FZD5 A219Xfs*49 may act as a secreted Frizzled-related protein (36). This acquired secretory function may act non-cell autonomously and antagonize WNT-FZD5 activity expressed from the wild type allele. To test this hypothesis, a co-culture assay was developed in which constructs A219Xfs*49 and Wnt9b plus FZD5 were respectively transfected into HEK293 and STF cells containing a built-in TCF luciferase reporter. Measurement of luciferase activity (schematically illustrated in Fig. 4A, left panel) revealed dose-dependent, non-cell autonomous inhibition of FZD5-mediated canonical WNT activity with co-cultured A219Xfs*49 expressing cells (Fig. 4A, middle panel). Moreover, the inhibition was reversed in a dose-dependent manner by increasing FZD5 expression (Fig. 4A, right panel). Similar results were obtained in a Wnt5a/FZD5-induced RhoA activity assay (Fig. 4B-C), which is a measure of non-canonical WNT signaling. Taken together, these data suggest that the A219Xfs*49 mutant protein functions in a dominant, non-cell autonomous manner to repress FZD5 signaling.

Forced expression of FZD5 A219Xfs*49 in mouse retina leads to apical junction defects similar to those observed in Fzd5/8 compound mutants

Previous studies in mice demonstrated apical junction defects in the retinal pigment epithelium of *Fzd5*/*Fzd8* compound mutant retina, and these were likely to contribute to or cause abnormal neurogenesis and coloboma (32). To examine whether the A219Xfs*49 mutation can mimic a *FZD5* dominant loss-of-function, we overexpressed the FZD5-A219Xfs*49 mutation in mouse retina and evaluated FZD5-related downstream molecular events. Mutant constructs were electroporated into E13.5 mouse retina together with a constitutive Ub-GFP expression vector, and the retina was analyzed after 72 hrs of culture *in*

vitro. Consistent with apical junction defects in *Fzd5*$^{-/-}$;*Fzd8*$^{+/-}$ compound mutant mouse retina (32), the overexpression of the A219Xfs*49 mutant also caused apical junction defects in cultured retinal explants, as indicated by attenuated expression of atypical Protein Kinase C (aPKC) (Fig. 5 A-F) and RhoA (Fig. 5 G-L). Both FZD5 and aPKC are expressed in retinal progenitor cells (see Fig. 5 and refs. (27, 32)). Decreased expression of these proteins likely represents the loss of concentrated apical localization of markers, which would not be demonstrated by immunoblotting. Furthermore, both human and mouse FZD5 showed the same apical retinal localization (Fig. 5M-R), supporting the hypothesis that they may mediate similar molecular events during human and mouse retinal development.

DISCUSSION

In the present study, we have identified an ultra-rare frameshift mutation in *FZD5* in a large extended family with non-syndromic coloboma segregating as an autosomal dominant disorder. The open reading frame of *FZD5* is entirely within the second exon which makes it unlikely that transcript would be subject to nonsense mediated decay since there is no intron-exon boundary 3' to the premature termination codon (37). The distinct location of the frameshift in the open reading frame suggests that the truncated protein would have an antagonistic effect on WNT signaling. This predicted effect was demonstrated in cultured cells, zebrafish retina and mouse retinal explants that establish *FZD5* as a strong candidate for human eye malformation(s).

FZD5 mutations with similar predicted dominant negative effect appear to be extremely rare in human populations. A total of 18 copy number variations (CNVs) encompassing *FZD5* locus are listed in DECIPHER database. Three patients with CNVs have eye abnormalities including cataract (one duplication case) and iris and/or chorioretinal coloboma (two deletion cases). However, a simple phenotype-genotype correlation could not be inferred since the CNV regions are large and include many genes. Only two *FZD5* "loss-of-function" alleles, both frameshift, are documented in ExAC. One of these, p.E231Afs*8 is also predicted to generate a secreted WNT-ligand binding domain with no transmembrane

domain. No phenotype information is available for the single individual carrying this mutation in a heterozygous state. Given that non-penetrance has been observed in at least two members of the family presented above, it is possible that this individual is non-penetrant or has microphthalmia, a disorder characterized by reduced ocular size that is closely associated with coloboma. An explanation for the rarity of such mutations may be related to the observation that *Fzd5* null mouse embryos die before E11 due to placental angiogenesis defects (38). The non-penetrance of such variants may reflect rescue via genetic background effects and/or compensation by paralogs. The latter effect is prominent in *Fzd5*/*Fzd8* mutant mice (32) although no obvious *FZD8* mutations compatible with a digenic effect were identified in WES in the individuals presented here. Notably, similar non-penetrance has been observed in patients with autosomal dominant coloboma due to *YAP1* (12) and *SHH* (8) mutation.

Our results demonstrate a direct role for WNT-FZD signaling in optic fissure closure during human eye development. The A219Xfs*49 mutation converts FZD5 from a membrane-bound WNT receptor to a secreted frizzled antagonist that, by competing with WNT ligands or dimerization with wild type FZD5 (on the cell surface), might impart dominant-negative characteristics on WNT signaling. As a result of the disrupted WNT signaling, retinal neuroblasts exhibit apical junction defects (Supplementary Fig. 8) (32), which could directly or indirectly impact proliferation, survival and maturation of progenitors (Supplementary Fig. 8), leading to microphthalmia and coloboma. The dominant-negative role of A219Xfs*49 mutant is also consistent with the absence of observable ocular defects in heterozygous *Fzd5* null allelic mice.

To date, ocular disorders attributable to mutations in WNT signaling are Norrie disease (16, 17), osteoporosis-pseudoglioma syndrome (18) and familial exudative vitreoretinopathy (16, 17, 19-21). Our study directly implicates perturbed WNT signaling in coloboma and microphthalmia and is consistent with conclusions from mouse models (23, 27, 32, 33). FZD5 mediates both canonical and non-canonical Wnt signaling pathways in different organisms and tissues (22, 27, 30). However, it is likely that FZD5-mediated non-

canonical WNT signaling is the predominant pathway in the developing mammalian retina, as only minimal activity from the canonical pathway has been reported in these cells (39). The retinal apical junction defects observed in *Fzd*5/*Fzd8*-knockout mice, and retinal explants expressing the FZD5 mutant protein are likely to be the consequence of interactions between the actin cytoskeleton and components of the apical junctional complexes induced by the loss of non-canonical Wnt activity. The identification of *FZD5* as a human coloboma gene extends opportunities to elucidate disease mechanisms and treatment paradigms for ocular malformations.

MATERIALS AND METHODS

Animal experiments

Animal Care and Use Committee of the National Eye Institute approved all procedures involving the use of mice. Fzd5 and Fzd8 compound mutants were created and maintained as described previously (32).

All zebrafish experiments were consistent with Canadian Council of Animal Care guidelines and approved by the University of Alberta's Animal Care and Use Committee (Protocol #427). Experiments utilized the wildtype AB zebrafish strain or Tg(TOP:dGFP)w25 transgenic strain (40). All embryos were grown at 28.5°C and staged according to developmental hallmarks (41).

Zebrafish morpholino and FZD5 mRNA injection experiments

Morpholino oligonucleotides (MO; GeneTools) were appropriately diluted in Danieau's solution, then heated to 65°C for 10 min and allowed to cool before injection into the 1-2 cell stage embryos. A previously described translation blocking MO targeting fzd5 (GATGCTCGTCTGCAGGTTTCCTCAT) was injected at a dose of 1.2 pmol (22). Morphological phenotypes were recapitulated by injecting a minimally overlapping MO (TGCAGGTTTCCTCA-TACTGGAAAGC) (data not shown). Human *FZD5* WT and *A219Xfs*49* cDNA was amplified using pRK5 constructs as template (see below) using the

following primer sequences: F – CACAGGATCCACCATGGCTCGGCCTG), R – CACAGAATTCCCTGAACCAAGTGGAA. PCR products were cloned into pCR4-TOPO (Invitrogen) for sequencing confirmation and sub-cloned into pCS2+ for mRNA synthesis. Constructs were linearized with NsiI (New England Biolabs) and mRNA was generated using the SP6 mMessage mMachine kit (Ambion). mRNA was purified using YM-50 Microcon columns (Amicon, Millipore) and the concentration was determined through spectrophotometry. The mRNA was diluted with DEPC-treated water and injected at a dose of 200pg into 1-cell stage embryos.

Whole mount in situ hybridization, immunofluorescence and live imaging

Live zebrafish embryos were photographed using an Olympus stereoscope with a Qimaging micropublisher camera. Whole mount in situ hybridization was performed as previously described (42). RT-PCR was used to generate 800-1200bp templates for probe synthesis or sub-cloned into pCR4-TOPO (Invitrogen). Immunofluorescence was performed as previously described (26) using rabbit polyclonal specific for Laminin (1/100) (Sigma L9393). After either *in situ* hybridization or immunofluorescence, eyes were dissected off and flat mounted for imaging on Zeiss AxioImager Z1 compound microscope with Axiocam HR digital camera.

Patients and DNA sequencing

Individuals with microphthalmia, anophthalmia and/or coloboma (MAC) were subjected to exome sequencing and Sanger sequencing. Genomic DNA samples fromcoloboma probands were analyzed by the National Eye Institute clinical eye center, UK10K consortium, MRC Human Genetics Unit at the IGMM, University of Edinburgh, and the University of Alberta. Informed consent was obtained from each participant, and study approval provided by the relevant ethics boards (NIH IRB; U of A Health Research Ethics Board (Reference # 01227), UK Multiregional Ethics Committee (Reference # 06/MRE00/76)). Five affected individuals from family 3483 (UK10K) were subjected to whole exome sequencing, and Sanger sequencing was used to test for the *FZD5* mutation in all other available members of

this branch of the family. Four affected individuals from family 111 (HREB) were Sanger sequenced for the *FZD5* gene. Exome sequencing was performed as described (43) with BWA 0.5.9 used for alignment, Picard 1.43 for duplicate marking, GATK 1.0.5506 for realignment around indels and base quality scores recalibration, and GATK Unified Genotyper for variant calling. LOD score was calculated using paramlink package in R (44). The oligonucleotides used to PCR amplify *FZD5* are listed in supplementary table 2.

Immunoblotting, immunofluorescence staining, and immunohistochemistry

For examining expression of FZD5 mutant constructs, plasmid DNA of each mutant (D97V or A219Xfs*49) or wild type FZD5 construct was transfected into HEK293T cells cultured in 6-well dishes. A total of 2 μg DNA was used for transfection for each well, and biological and technical triplicates were made for each transfection. Transfected ells were cultured for 36 hr, supplemented with serum reduced medium (Opti-MEM, life technologies, Cat. #31985), continually cultured for another 24 hr. Cell medium was collected and store at -800C. Total cell extracts were prepared by adding 2XSDS Laemmli buffer (BIO-RAD, cat. #161-0737) onto cells rinsed with PBS. To prepare extracellular matrix (ECM) proteins, cultured cells were washed with PBS and incubated in PBS containing 10mm EDTA at 37°C for 30-45 min to remove the cells. ECM proteins are retained on the dish and solubilized in Laemmli buffer.

Immunoblotting was performed as described previously (32) using custom-made rabbit antibody against the N-terminus 143 residues (27-169 amino acids) of the mouse FZD5 protein. The signal intensities were quantified by NIH ImageJ from three representative Western blots, and analyzed by Microsoft Excel. To detect FZD5 and FZD5 A219Xfs*49 cellular or extracellular localization, two μg DNA was used for transfection in each well (6-well plate) carrying coated coverslips. Transfected cells were cultured in DMEM-F12 for 48 hr. Immunofluorescence staining was conducted using the same antibody for detection of mutated/variant FZD5 proteins. To avoid cytoplasmic staining, live cells were first incubated with anti-Fzd5 antibody in cultured medium at 40°C for 2 hr, washed with PBS,

and then post-fixed with PFA. After rinse with PBS, secondary antibody was added to further proceed with immunohistochemistry. Standard immunohistochemistry was performed on PFA-fixed frozen retinal sections with anti-Fzd5 antibody (1:500), anti-aPKC (1:500, cell signaling, Cat. # 9378) and anti-RhoA (Cytoskeleton, Cat. # ARH03).

FZD5 gene mutagenesis and Wnt/beta-catenin pathway activation assay

FZD5 cDNA was cloned into pRK5 expression vector with a CMV promoter and site-directed mutagenesis was performed to generate the FZD5 A219Xfs*49 frameshift mutation. For testing canonical Wnt signaling activity, DNA constructs were transfected into STF HEK 293 cells with a 7XTCF promoter-driven firefly luciferase reporter stably integrated in the genome (27). As shown in Fig. 4A, fixed amount of Wnt9b and FZD5 were cotransfected together with pCAG-renilla luciferase plasmids (RL, used for internal expression control) into STF cells. Different amount of FZD5 A219Xfs*49 and sCRD plasmids were transfected into regular HEK293 cells, respectively. Twelve hours after transfection, both STF and HEK293 cells were lifted off by trypsin-EDTA, and mixed at 1:1 ratio and seeded into new plate for another 36hr culture. Biological and technical triplicates were prepared for each transfection. Cell extracts were then prepared for Firefly luciferase and renilla luciferase assay using Dual-luciferase assay system (Promega, E1960). Luminicence was measured sequentially by Turner Biosystem Modulus microplate reader. Firefly luciferase activity was normalized against renilla luciferase, and p-value calculation was performed using Microsoft Excel software student t-test function.

Active RhoA assay for Wnt5 a stimulation

HEK293 cells were cultured to 80% confluence in DMEM:F12 in 6-well dishes, transfected with FZD5 WT, A219Xfs*49 and sCRD plasmids, cultured for 24 hrs, then serum starved for 24 hrs. Wnt5a recombinant protein conditioned medium (Wnt5a CM, Roche, Cat: 645-WN-010/CF) was applied for 30min at 250ng/ml. Cells were lysed and then subjected to active GTP-RhoA assays according to the manufacturer instructions (pulldown assay:

RhoA/Rac1/Cdc42 assay kit, Cytoskeleton Inc, cat. # Bk- 030; G-lisa assay: RhoA G-lisa kit, Cytoskeleton Inc, cat. # Bk-124). Signal intensity was acquired by NIH ImageJ from three representative immunoblots. Light absorbance/optic density of HRP colorimetric reaction was measured (SpectraMax M), and the data was analyzed in Microsoft Excel.

Retinal electroporation and explants culture

Mouse embryonic retinas were dissected in DMEM medium at E13.5 excluding lens and RPE. Retinae were subjected to electroporation with BTX ECM830 electroporator in embryo GPS chamber (SunIVF, EGPS-010) supplied with 250 ng/μl DNA solution in1XPBS. The following parameters were set for electroporation: 21 volts for electric field strength; 5X current pulses (50 ms duration); 900ms intervals between pulses. Retinas were then cultured in DMEM:F12 (Invitrogen, Cat. 12660-012) for 72 hr, harvested in PBS and fix in 4% PFA, and subjected to sectioning and immunohistochemistry (32).

Co-immunoprecipitation (Co-IP)

HEK293T cells were transfected with 1.5 μg DNA in each well of a 6-well dishe. Myc-tagged *Wnt3a*, HA-tagged *WNT7A* were coexpressed, respectively, with FZD5 or FZD5A219X49. Cell extracts and Co-IP procedure were performed essentially as described (34). Antibodies used were mouse anti-HA (TransGene Biotech, HT301), rabbit anti-myc (Sigma, C3956), and rabbit anti-FZD5 (custom-made). Protein A agarose resin was purchased from TansGene Biotech (DP301).

ACKNOWLEDGMENTS

We are grateful to Jeremy Nathans for WNT-FZD constructs and reporter cell lines. We thank Arvydas Maminishkis for providing human fetal retina and Suja Hiriyanna for technical assistance. These studies were supported by Intramural Research program of the National Eye Institute (AS, TL, BB), a UK Medical Research Council block grant to the University of Edinburgh MRC Human Genetics Unit (DRF, KAW, JR), and by grants from NSERC, AITF and WCHRI (SAW, AJW), CIHR and WCHRI (OJL), and 100 People Plan of Sun Yat-sen University (CL). The Welcome Trust supported UK10K project (#WT091310).

Conflict of interest

The authors claim no conflict of interest for publishing this study.

REFERENCES

1 Hornby, S.J., Gilbert, C.E., Rahi, J.K., Sil, A.K., Xiao, Y., Dandona, L. and Foster, A. (2000) Regional variation in blindness in children due to microphthalmos, anophthalmos and coloboma. *Ophthalmic Epidemiol*, **7**, 127-138.

2 Gregory-Evans, C.Y., Williams, M.J., Halford, S. and Gregory-Evans, K. (2004) Ocular coloboma: a reassessment in the age of molecular neuroscience. *J Med Genet*, **41**, 881-891.

3 Williamson, K.A. and FitzPatrick, D.R. (2014) The genetic architecture of microphthalmia, anophthalmia and coloboma. *Eur J Med Genet*, **57**, 369-380.

4 Bakrania, P., Efthymiou, M., Klein, J.C., Salt, A., Bunyan, D.J., Wyatt, A., Ponting, C.P., Martin, A., Williams, S., Lindley, V. *et al.* (2008) Mutations in BMP4 cause eye, brain, and digit developmental anomalies: overlap between the BMP4 and hedgehog signaling pathways. *Am J Hum Genet*, **82**, 304-319.

5 Rainger, J., van Beusekom, E., Ramsay, J.K., McKie, L., Al-Gazali, L., Pallotta, R., Saponari, A., Branney, P., Fisher, M., Morrison, H. *et al.* (2011) Loss of the BMP antagonist, SMOC-1, causes Ophthalmo-acromelic (Waardenburg Anophthalmia) syndrome in humans and mice. *PLoS Genet*, **7**, e1002114.

6 Wyatt, A.W., Osborne, R.J., Stewart, H. and Ragge, N.K. (2010) Bone morphogenetic protein 7 (BMP7) mutations are associated with variable ocular, brain, ear, palate, and skeletal anomalies. *Hum Mutat*, **31**, 781-787.

7 Asai-Coakwell, M., French, C.R., Berry, K.M., Ye, M., Koss, R., Somerville, M., Mueller, R., van Heyningen, V., Waskiewicz, A.J. and Lehmann, O.J. (2007) GDF6, a novel locus for a spectrum of ocular developmental anomalies. *Am J Hum Genet*, **80**, 306-315.

8 Schimmenti, L.A., de la Cruz, J., Lewis, R.A., Karkera, J.D., Manligas, G.S., Roessler, E. and Muenke, M. (2003) Novel mutation in sonic hedgehog in non-syndromic colobomatous microphthalmia. *Am J Med Genet A*, **116A**, 215-221.

9 Pasutto, F., Sticht, H., Hammersen, G., Gillessen-Kaesbach, G., Fitzpatrick, D.R., Nurnberg, G., Brasch, F., Schirmer-Zimmermann, H., Tolmie, J.L., Chitayat, D. *et al.* (2007) Mutations in STRA6 cause a broad spectrum of malformations including anophthalmia, congenital heart defects, diaphragmatic hernia, alveolar capillary dysplasia, lung hypoplasia, and mental retardation. *Am J Hum Genet*, **80**, 550-560.

10 Srour, M., Chitayat, D., Caron, V., Chassaing, N., Bitoun, P., Patry, L., Cordier, M.P., Capo-Chichi, J.M., Francannet, C., Calvas, P. *et al.* (2013) Recessive and dominant mutations in retinoic acid receptor beta in cases with microphthalmia and diaphragmatic hernia. *Am J Hum Genet*, **93**, 765-772.

11 Fares-Taie, L., Gerber, S., Chassaing, N., Clayton-Smith, J., Hanein, S., Silva, E., Serey, M., Serre, V., Gerard, X., Baumann, C. *et al.* (2013) ALDH1A3 mutations cause recessive anophthalmia and microphthalmia. *Am J Hum Genet*, **92**, 265-270.

12 Williamson, K.A., Rainger, J., Floyd, J.A., Ansari, M., Meynert, A., Aldridge, K.V., Rainger, J.K., Anderson, C.A., Moore, A.T., Hurles, M.E. *et al.* (2014) Heterozygous loss-of-function mutations in YAP1 cause both isolated and syndromic optic fissure closure defects. *Am J Hum Genet*, **94**, 295-302.

13 Ye, M., Berry-Wynne, K.M., Asai-Coakwell, M., Sundaresan, P., Footz, T., French, C.R., Abitbol, M., Fleisch, V.C., Corbett, N., Allison, W.T. *et al.* (2010) Mutation of the bone morphogenetic protein GDF3 causes ocular and skeletal anomalies. *Hum Mol Genet*, **19**, 287-298.

14 Morcillo, J., Martinez-Morales, J.R., Trousse, F., Fermin, Y., Sowden, J.C. and Bovolenta, P. (2006) Proper patterning of the optic fissure requires the sequential activity of BMP7 and SHH. *Development*, **133**, 3179-3190.

15 Reis, L.M., Tyler, R.C., Schilter, K.F., Abdul-Rahman, O., Innis, J.W., Kozel, B.A., Schneider, A.S., Bardakjian, T.M., Lose, E.J., Martin, D.M. *et al.* (2011) BMP4 loss-of-function mutations in developmental eye disorders including SHORT syndrome. *Hum Genet*, **130**, 495-504.

16 Chen, Z.Y., Battinelli, E.M., Fielder, A., Bundey, S., Sims, K., Breakefield, X.O. and Craig, I.W. (1993) A mutation in the Norrie disease gene (NDP) associated with X-linked familial exudative vitreoretinopathy. *Nat Genet*, **5**, 180-183.

17 Nikopoulos, K., Venselaar, H., Collin, R.W., Riveiro-Alvarez, R., Boonstra, F.N., Hooymans, J.M., Mukhopadhyay, A., Shears, D., van Bers, M., de Wijs, I.J. *et al.* (2010) Overview of the mutation spectrum in familial exudative vitreoretinopathy and Norrie disease with identification of 21 novel variants in FZD4, LRP5, and NDP. *Hum Mutat*, **31**, 656-666.

18 Gong, Y., Slee, R.B., Fukai, N., Rawadi, G., Roman-Roman, S., Reginato, A.M., Wang, H., Cundy, T., Glorieux, F.H., Lev, D. *et al.* (2001) LDL receptor-related protein 5 (LRP5) affects bone accrual and eye development. *Cell*, **107**, 513-523.

19 Robitaille, J., MacDonald, M.L., Kaykas, A., Sheldahl, L.C., Zeisler, J., Dube, M.P., Zhang, L.H., Singaraja, R.R., Guernsey, D.L., Zheng, B. *et al.* (2002) Mutant frizzled-4 disrupts retinal angiogenesis in familial exudative vitreoretinopathy. *Nat Genet*, **32**, 326-330.

20 Toomes, C., Bottomley, H.M., Jackson, R.M., Towns, K.V., Scott, S., Mackey, D.A., Craig, J.E., Jiang, L., Yang, Z., Trembath, R. *et al.* (2004) Mutations in LRP5 or FZD4 underlie the common familial exudative vitreoretinopathy locus on chromosome 11q. *Am J Hum Genet*, **74**, 721-730.

21 Poulter, J.A., Davidson, A.E., Ali, M., Gilmour, D.F., Parry, D.A., Mintz-Hittner, H.A., Carr, I.M., Bottomley, H.M., Long, V.W., Downey, L.M. *et al.* (2012) Recessive mutations in TSPAN12 cause retinal dysplasia and severe familial exudative vitreoretinopathy (FEVR). *Invest Ophthalmol Vis Sci*, **53**, 2873-2879.

22 Cavodeassi, F., Carreira-Barbosa, F., Young, R.M., Concha, M.L., Allende, M.L., Houart, C., Tada, M. and Wilson, S.W. (2005) Early stages of zebrafish eye formation require the coordinated activity of Wnt11, Fz5, and the Wnt/beta-catenin pathway. *Neuron*, **47**, 43-56.

23 Hagglund, A.C., Berghard, A. and Carlsson, L. (2013) Canonical Wnt/beta-catenin signalling is essential for optic cup formation. *PLoS One*, **8**, e81158.

24 Lieven, O. and Ruther, U. (2011) The Dkk1 dose is critical for eye development. *Dev Biol*, **355**, 124-137.

25 Veien, E.S., Rosenthal, J.S., Kruse-Bend, R.C., Chien, C.B. and Dorsky, R.I. (2008) Canonical Wnt signaling is required for the maintenance of dorsal retinal identity. *Development*, **135**, 4101-4111.

26 Holly, V.L., Widen, S.A., Famulski, J.K. and Waskiewicz, A.J. (2014) Sfrp1a and Sfrp5 function as positive regulators of Wnt and BMP signaling during early retinal development. *Dev Biol*, **388**, 192-204.

27 Liu, C. and Nathans, J. (2008) An essential role for frizzled 5 in mammalian ocular development. *Development*, **135**, 3567-3576.

28 Borello, U., Buffa, V., Sonnino, C., Melchionna, R., Vivarelli, E. and Cossu, G. (1999) Differential expression of the Wnt putative receptors Frizzled during mouse somitogenesis. *Mech Dev*, **89**, 173-177.

29 Sumanas, S. and Ekker, S.C. (2001) Xenopus frizzled-5: a frizzled family member expressed exclusively in the neural retina of the developing eye. *Mech Dev*, **103**, 133-136.

30 Van Raay, T.J., Moore, K.B., Iordanova, I., Steele, M., Jamrich, M., Harris, W.A. and Vetter, M.L. (2005) Frizzled 5 signaling governs the neural potential of progenitors in the developing Xenopus retina. *Neuron*, **46**, 23-36.

31 Burns, C.J., Zhang, J., Brown, E.C., Van Bibber, A.M., Van Es, J., Clevers, H., Ishikawa, T.O., Taketo, M.M., Vetter, M.L. and Fuhrmann, S. (2008) Investigation of Frizzled-5 during embryonic neural development in mouse. *Dev Dyn*, **237**, 1614-1626.

32 Liu, C., Bakeri, H., Li, T. and Swaroop, A. (2012) Regulation of retinal progenitor expansion by Frizzled receptors: implications for microphthalmia and retinal coloboma. *Hum Mol Genet*, **21**, 1848-1860.

33 Zhou, C.J., Molotkov, A., Song, L., Li, Y., Pleasure, D.E., Pleasure, S.J. and Wang, Y.Z. (2008) Ocular coloboma and dorsoventral neuroretinal patterning defects in Lrp6 mutant eyes. *Dev Dyn*, **237**, 3681-3689.

34 Carmon, K.S. and Loose, D.S. (2008) Secreted frizzled-related protein 4 regulates two Wnt7a signaling pathways and inhibits proliferation in endometrial cancer cells. *Mol Cancer Res*, **6**, 1017-1028.

35 Carmon, K.S. and Loose, D.S. (2010) Development of a bioassay for detection of Wnt-binding affinities for individual frizzled receptors. *Anal Biochem*, **401**, 288-294.

36 Bodine, P.V., Zhao, W., Kharode, Y.P., Bex, F.J., Lambert, A.J., Goad, M.B., Gaur, T., Stein, G.S., Lian, J.B. and Komm, B.S. (2004) The Wnt antagonist secreted frizzled-related protein-1 is a negative regulator of trabecular bone formation in adult mice. *Mol Endocrinol*, **18**, 1222-1237.

37 Popp, M.W. and Maquat, L.E. (2013) Organizing principles of mammalian nonsense-mediated mRNA decay. *Annu Rev Genet*, **47**, 139-165.

38 Ishikawa, T., Tamai, Y., Zorn, A.M., Yoshida, H., Seldin, M.F., Nishikawa, S. and Taketo, M.M. (2001) Mouse Wnt receptor gene Fzd5 is essential for yolk sac and placental angiogenesis. *Development*, **128**, 25-33.

39 Liu, H., Thurig, S., Mohamed, O., Dufort, D. and Wallace, V.A. (2006) Mapping canonical Wnt signaling in the developing and adult retina. *Invest Ophthalmol Vis Sci*, **47**, 5088-5097.

40 Dorsky, R.I., Sheldahl, L.C. and Moon, R.T. (2002) A transgenic Lef1/beta-catenin-dependent reporter is expressed in spatially restricted domains throughout zebrafish development. *Dev Biol*, **241**, 229-237.

41 Kimmel, C.B., Ballard, W.W., Kimmel, S.R., Ullmann, B. and Schilling, T.F. (1995) Stages of embryonic development of the zebrafish. *Dev Dyn*, **203**, 253-310.

42 Gongal, P.A. and Waskiewicz, A.J. (2008) Zebrafish model of holoprosencephaly demonstrates a key role for TGIF in regulating retinoic acid metabolism. *Hum Mol Genet*, **17**, 525-538.

43 Olbrich, H., Schmidts, M., Werner, C., Onoufriadis, A., Loges, N.T., Raidt, J., Banki, N.F., Shoemark, A., Burgoyne, T., Al Turki, S. *et al.* (2012) Recessive HYDIN mutations cause primary ciliary dyskinesia without randomization of left-right body asymmetry. *Am J Hum Genet*, **91**, 672-684.

44 Egeland, T., Pinto, N. and Vigeland, M.D. (2014) A general approach to power calculation for relationship testing. *Forensic Sci Int Genet*, **9**, 186-190.

LEGENDS TO FIGURES

Figure 1. A *FZD5* frameshift mutation identified in a family with autosomal dominant coloboma

A, Six- and three-generation family pedigrees of Family 3483 and Family 111, respectively. The dotted line links these independently ascertained pedigrees carrying the same mutation on an identical haplotype. This link is plausible based on the history obtained from both Mennonite families, with the likely linking individual (Family 3483 II:4) having emigrated from Europe to North America. For Family 3483, ocular images from the affected individuals are shown adjacent to the cognate pedigree symbol. COL numbers indicate individuals whose exomes were sequenced. Otherwise, Sanger sequencing was used for segregation analysis, which reveals high (0.8) but incomplete penetrance, as indicated by two obligate carriers that are unaffected. The pedigree key is in the top left corner. B, Representative images showing eye malformations in affected individuals from Family 111. The LOD score for the combined pedigree is shown below the family tree. C, Chromatopherogram of the frameshift *FZD5* mutation (c.656delCinsAG). D, Schematic of the human *FZD5* gene with hg19 coordinates on chromosome 2. This gene is transcribed in the antisense direction relative to the genomic coordinate numbering. The position of the cDNA mutation is indicated in the open reading frame (ORF), which is entirely contained in the second exon. Below are diagrammatic representations of the wild type and “mutant” FZD5 peptides. The WNT binding domain (dark blue box) is common to both, and the seven transmembrane domains (orange boxes) are present only in the wild type protein of 585 residues. The mutation results in the truncation at Ala219 (substituted to Glu) with an aberrant extension of 48 residues (red box), resulting in a protein of 266 amino acids.

Figure 2. Morpholino knockdown and over-expression of *FZD5* causes microphthalmia and coloboma in zebrafish.

A-B, Representative images of live embryos at 3 dpf, either uninjected (A) or injected with 1.2 pmol of *fzd5* translation blocking morpholino (MO; B). C-D, In situ hybridization for *GFP* was performed at 28 hpf in *Tg[TOP:dGFP]* embryos to assess levels of canonical Wnt signaling in uninjected (C; n=26/26 eyes) or *fzd5* morphants (D; n=23/25 eyes). Retinal *GFP* expression was increased in morphants, while lens expression was decreased (D compare to C), suggesting a tissue-specific function for *fzd5* in Wnt signaling. E-L, Embryos were injected at the 1-cell stage with either 200 pg human WT *FZD5* mRNA or *A219Xfs*49 FZD5* mRNA and imaged to analyze eye size and prevalence of coloboma. Injection of WT *FZD5* caused higher incidence of microphthalmia (K, ***, p<0.0002) and coloboma (L, **, p=0.016; *, p=0.008) compared to injection of *A219Xfs*49 FZD5* mRNA. All images represent majority of observed phenotypes in each injection group. E-G, Live images of larvae at 3 dpf; H-J, eyes labeled with β-laminin antibody at 3 dpf. K-L, Quantification of ocular phenotypes seen in E-J. For E-L, Number of embryos analyzed for microphthalmia: uninjected (n=85), WT *FZD5* (n=34), *A219Xfs*49* (n=67), 2 experimental replicates. Number of embryos analyzed for coloboma: uninjected (n=54), WT *FZD5* (n=20), *A219Xfs*49* (n=54), 2 experimental replicates.

Figure 3. FZD5-A219Xfs*49 is incapable of mediating Wnt signaling

A, Immunoblot analysis of subcellular fractions from transfected HEK293 cells. FZD5 A219Xfs*49mutant protein is detected primarily in extracellular matrix (ECM) fraction. Secreted Cysteine-rich domain (sCRD) is expressed in both culture medium (CM) and ECM. CE: cell extract. B, Live cell immunofluorescence detection. Immunofluorescence staining was conducted to detect FZD5 proteins expression in transfected cells on coated coverslips (see materials and methods). WT FZD5 is primarily present on the cell surface (left panel),

whilst majority of A219Xfs*49 mutant protein is detected extracellularly (middle panel), presumptively in ECM (doted staining). Negative control with vector transfection is shown in the right panel. C, Wnt9b-induced canonical Wnt signaling in SupertopFlash (STF) reporter cell line. Cells were transfected with 0.5ug Wnt9b plasmid combined with 0.25ug other plasmids. Like sCRD, FZD5 A219Xfs*49 mutant protein is not able to mediate Wnt9b-induced canonical Wnt signaling. The rightmost bar represents Wnt9b-induced canonical Wnt activity by wild type FZD5, which is significantly different from all other froms of FZD5. D, Representative image foractive-Rho pulldown assays for non-canonical Wnt signaling. HEK293 cells were transfected with FZD5 WT, A219Xfs*49 and sCRD plasmids, treated with Wnt5a recombinant protein conditioned medium. Active GTP-RhoA assays strictly followed the manufacturer instructions (Cytoskeleton Inc, cat. # Bk-030) (details see materials and methods). Wnt5a-enhanced formation of GTP-RhoA is obtained in the presence of FZD5, but not A219Xfs*49 mutant or sCRD. The signal intensities were quantified by NIH ImageJ from three immunoblots for three independent experiments, and analyzed by Microsoft Excel (Student t-test, ***, $p<0.001$).

Figure 4. Non-cell autonomous dominant-negative effect of FZD5 A219Xfs*49 mutant on Wnt signaling.

A, Wnt9b-FZ5 signaling. All experiments were done in triplicates of at least three independent transfections. Left panel, illustration of the experimental scheme. A fixed amount of Wnt9b and FZD5 was co-transfected with pCAG-renilla luciferase plasmids (RL, used for internal expression control) into STF cells. Different amounts of FZD5 A219Xfs*49 and sCRD plasmids were transfected into HEK293 cells. After 12 hr, both STF and HEK293 cells were collected by trypsin-EDTA, mixed at 1:1 ratio, and seeded into a new plate for another 36 hr. Cell extracts were then prepared for Firefly luciferase and renilla luciferase assay. Middle Panel, inhibition of Wnt9b/FZD5 activity by either A219Xfs*49or sCRD in a dose-dependent manner. Firefly Luciferase activities were normalized against Renilla Luciferase, and statistics was performed using Microsoft Excel software. Right panel, the

inhibition of FZD5-mediated Wnt signaling by A219Xfs*49 or sCRD A219Xfs*49 or sCRD was reversed by augmenting FZD5 expression.

B, Wnt5a-FZD5 signaling. RhoA G-lisa assay showed that Wnt5a/FZD5-stimulated accumulation of GTP-RhoA was abolished by A219Xfs*49 mutant or sCRD protein (compare the right three bars). Samples preparation was as described in Fig. 3D, G-lisa assay followed instructions of RhoA G-lisa kit (Cytoskeleton Inc). Absorbance of HRP colorimetric reaction was measured by SpectraMax M. The data were quantified by Microsoft Excel.

C, Inhibition of RhoA activation by A219Xfs*49 or sCRD protein was reverted by increased FZD5 expression. Left panel: similar experimental scheme in 'A' was used for testing non-cell autonomous effects of A219Xfs*49 on Wnt5a/FZD5 induced RhoA activation. Right panel: The inhibition of RhoA activation (G-lisa assay) was reverted by increased FZD5 expression. ***, $p<0.001$, Student t-test.

Figure 5. Overexpression of FZD5 A219Xfs*49 led to similar apical junction defects that were reported in mouse Fz5/8 compound mutants.

Mouse embryonic (E13.5) retina was dissected and subjected to electroporation supplied with wild type FZD5 and FZD5 A219Xfs*49 DNA solution. The retinae were cultured for 72 hr and harvested for immunohistochemistry. A-F, aPKC localization in vector (A), wild type FZD5 (WT) (B) and A219Xfs*49 mutant (C) electroporated retinae. Note the loss of apical localization of aPKC in A219Xfs*49-expressing retina (C). D-F, Images of A, B, and C merged with coelctroporated eGFP, respectively. G-I, Similar as aPKC, apical RhoA enrichment is also greatly attenuated (compared to G and H). J-L, Images of G, H, and I merged with co-elctroporated eGFP, respectively. M-R, Localization of FZD5 protein in mouse and human retina. M, Apical localization of FZD5 protein in wild type mouse retina (above dashed bracket). N, Same protein localization of FZD5 was detected in human retina. O, Mouse *Fzd5* conditional mutant retina showed absence of apical FZD5 protein. P-R, Images from M-O merged with DAPI, respectively.

a.

Bilateral chorioretinal coloboma +/- iris colobma

Unilateral optic disc/nerve pigmentary abnormality

N Mutation not present

Mutation present

COL UK10K Exome sequence

1-32 Number in linkage table

Family 3483

I

II

III

IV

V

VI

1 I:1 2 I:2

3 II:1 4 II:2 5 II:3 6 II:4

7 III:1 8 III:2

emigrated from Volga region

>= 2 generations

IV:1 9 IV:1 10 IV:2 IV:3 IV:4 IV:5

IV:6 11 IV:6 COL5001064

no family history of coloboma

12 N IV:7 COL5103592

IV:7

V:1 13 V:1 COL5103591 14 V:2 V:3 V:4 V:5

V:6 15 V:6 16 V:7

17 V:8 18 V:9

VI:2 19 VI:1 VI:2 COL5001063 COL5103590 VI:3 VI:4

VI:5 20 VI:5 COL5103593 VI:6

VI:7 21 VI:7 22 N VI:8 VI:9

Family 111

28 I:1 27 I:2

29 II:1 3 II:2-4 31 II:5 30 II:6 II:7

32 III:1

b.

Family 111

Maximum LOD for combined family is 4.07 at θ = 0 penetrance = 0.8

c.

FZD5 c.656delCinsAG p.(Ala219Glufs*49)

215 Val Val Pro Pro Asn Asn Cys Cys Ala Ala/Glu 220 Val Val Pro Pro

565 570 575 580 G T G C C C A A C T G C G C G G T A C C C

435 440 445 450 G T G C C C A A C T G C G N G G N W M C C

d.

chr2:208628000 208630000 208632000 208634000

FZD5

exon 2 c.656delCinsAG exon 1

3'UTR ORF 5'UTR

transmembrane domains

1 585 FZD5

WNT binding domain

frameshift sequence

1 219 266 FZD5 p.Ala219Glufs*49

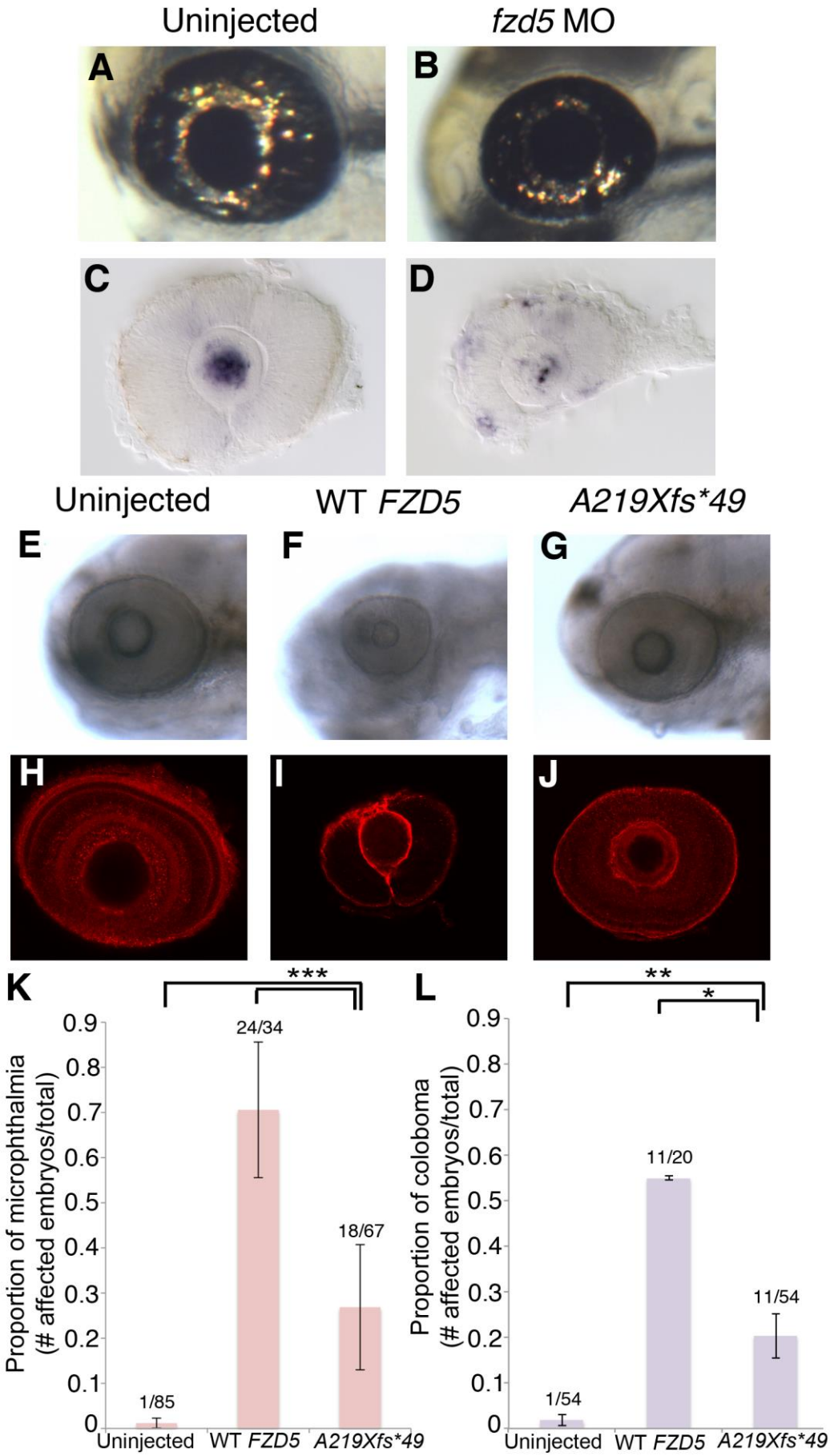

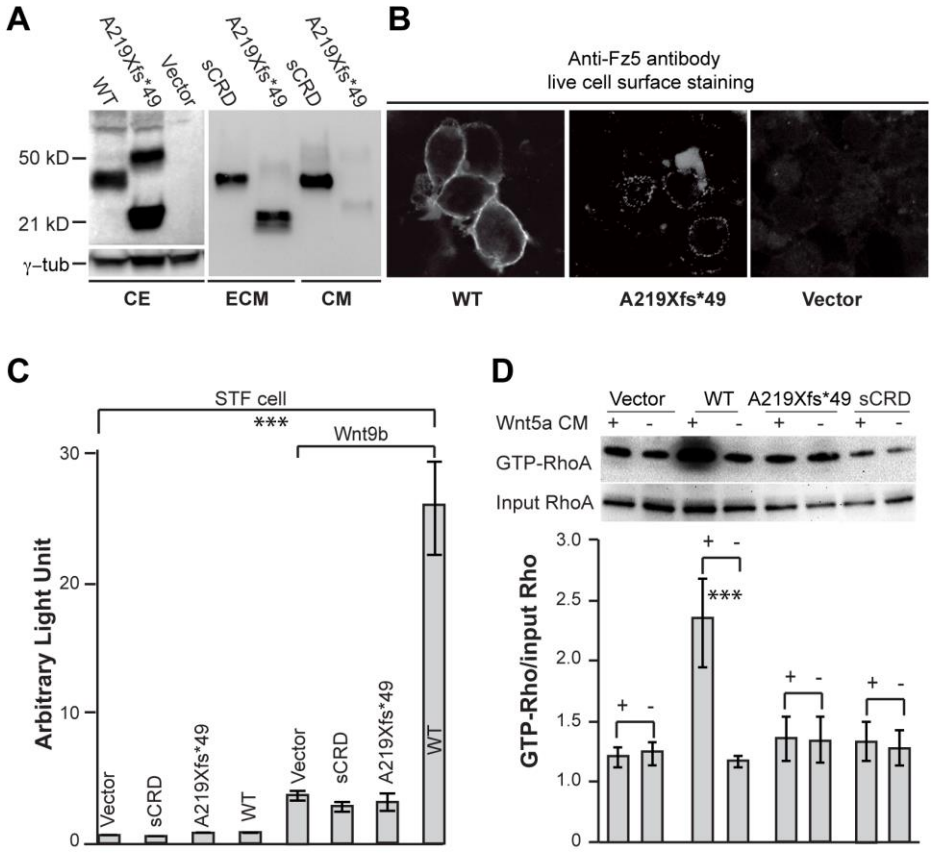

Figure 3

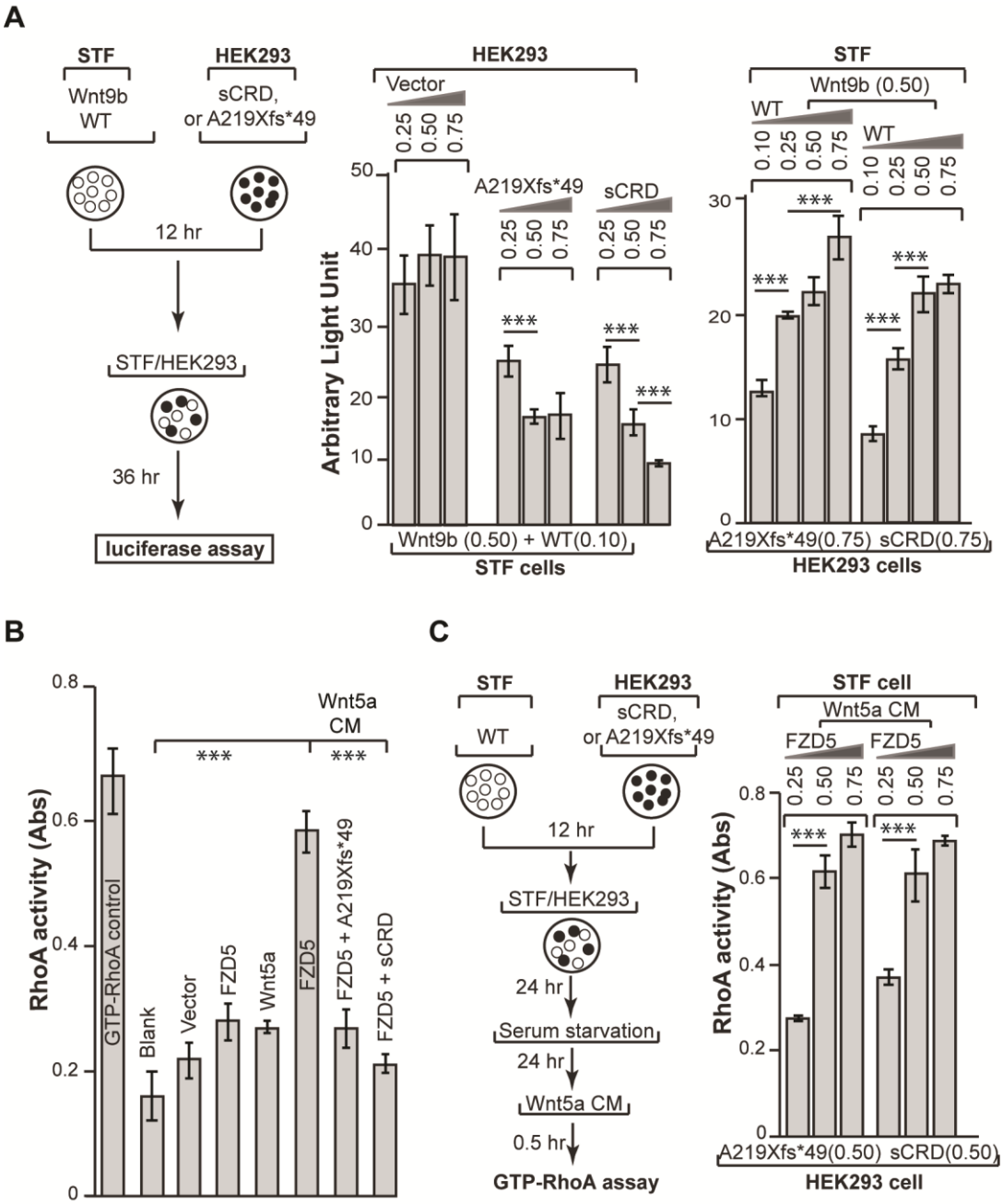

Figure 4

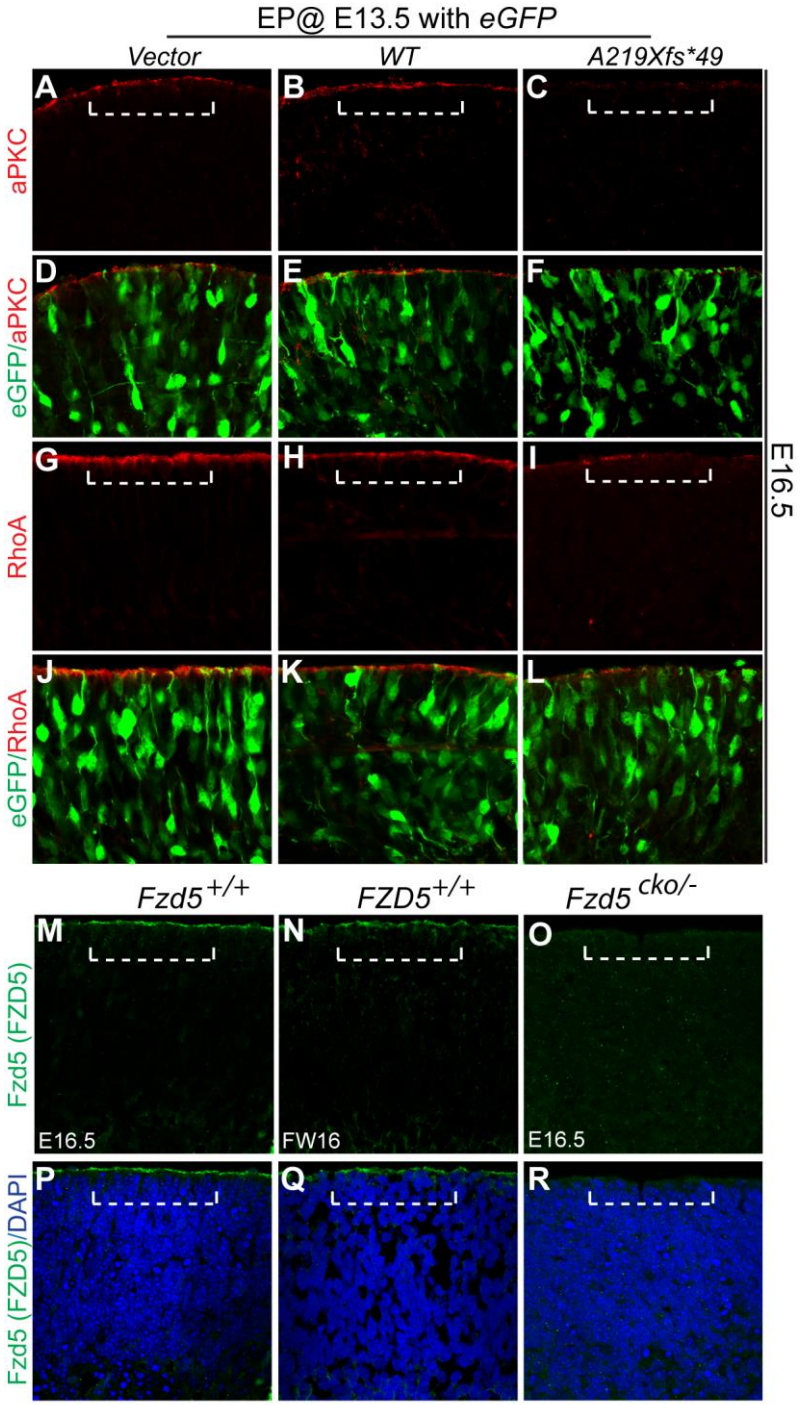

Figure 5